

Article

On the Performance of LDPC-Coded Massive MIMO Schemes with Power-Ordered NOMA Techniques

Mário Marques da Silva ^{1,2,3,*} , Rui Dinis ^{1,3,4}  and Gelson Martins ²¹ Instituto de Telecomunicações, 1049-001 Lisboa, Portugal; rdinis@fct.unl.pt² Department of Sciences and Technologies, Universidade Autónoma de Lisboa, 1169-023 Lisboa, Portugal; 30005668@students.ual.pt³ Autonomia TechLab, 1169-023 Lisboa, Portugal⁴ Faculty of Sciences and Technology, Universidade Nova, 2829-516 Caparica, Portugal

* Correspondence: mmsilva@autonomia.pt

Abstract: This article studies the power-ordered Non-Orthogonal Multiple Access (NOMA) techniques associated with Low-Density Parity-Check (LDPC) codes, adopted for use in the fifth generation of cellular communications (5G). Both conventional and cooperative NOMA are studied, associated with Single Carrier with Frequency Domain Equalization (SC-FDE) and massive Multiple-Input Multiple-Output (MIMO). Billions of Internet of Things (IoT) devices are aimed to be incorporated by the Fourth Industrial Revolution, requiring more efficient use of the spectrum. NOMA techniques have the potential to support that goal and represent strong candidates for incorporation into future releases of 5G. This article shows that combined schemes associated with both conventional and cooperative LDPC-coded NOMA achieve good performance while keeping the computational complexity at an acceptable level.

Keywords: NOMA; LDPC; massive MIMO; SC-FDE; 5G

Citation: Marques da Silva, M.; Dinis, R.; Martins, G. On the Performance of LDPC-Coded Massive MIMO Schemes with Power-Ordered NOMA Techniques. *Appl. Sci.* **2021**, *11*, 8684. <https://doi.org/10.3390/app11188684>

Academic Editor: Akram Alomainy

Received: 25 August 2021

Accepted: 13 September 2021

Published: 17 September 2021

Publisher's Note: MDPI stays neutral with regard to jurisdictional claims in published maps and institutional affiliations.



Copyright: © 2021 by the authors. Licensee MDPI, Basel, Switzerland. This article is an open access article distributed under the terms and conditions of the Creative Commons Attribution (CC BY) license (<https://creativecommons.org/licenses/by/4.0/>).

1. Introduction

The Fourth Industrial Revolution consists of the revolution of robots. Artificial intelligence is utilized to support the decision-making of robots, namely, to process a large amount of data (big data) that is generated with high data rate communications and using a wide variety of sensors and Internet of Things (IoT) devices. The Fourth Industrial Revolution is already deeply modifying humans and society in a myriad of areas, such as economy, mobility, housing, teaching, health, agriculture, medical and lawyer counselling, defense, wildlife monitoring, etc. [1,2].

From the communication and IoT point of view, the fifth generation of cellular communications (5G) was designed to offer the services required by the Fourth Industrial Revolution, representing a modification of the paradigm when compared to previous generations. One novelty of 5G relies on the ability to support direct device-to-device communication without requiring a base station, which is needed to support IoT devices required for autonomous vehicles, smart logistics, and smart cities. Moreover, as can be seen from Figure 1, to support different services with the required reliability, 5G is split into three groups of use cases: Enhanced Mobile Broadband (eMBB), massive Machine-Type Communications (mMTC) and Ultra-Reliable Low Latency Communications (URLLC). These three groups support the network slicing concept, which aims to provide diverse requirements for different users. For example, smart cities employ an extremely high number of devices with low power consumption, which is supported by mMTC. On the other side, autonomous vehicles require communication that is highly reliable and almost real-time, which is supported by URLLC.

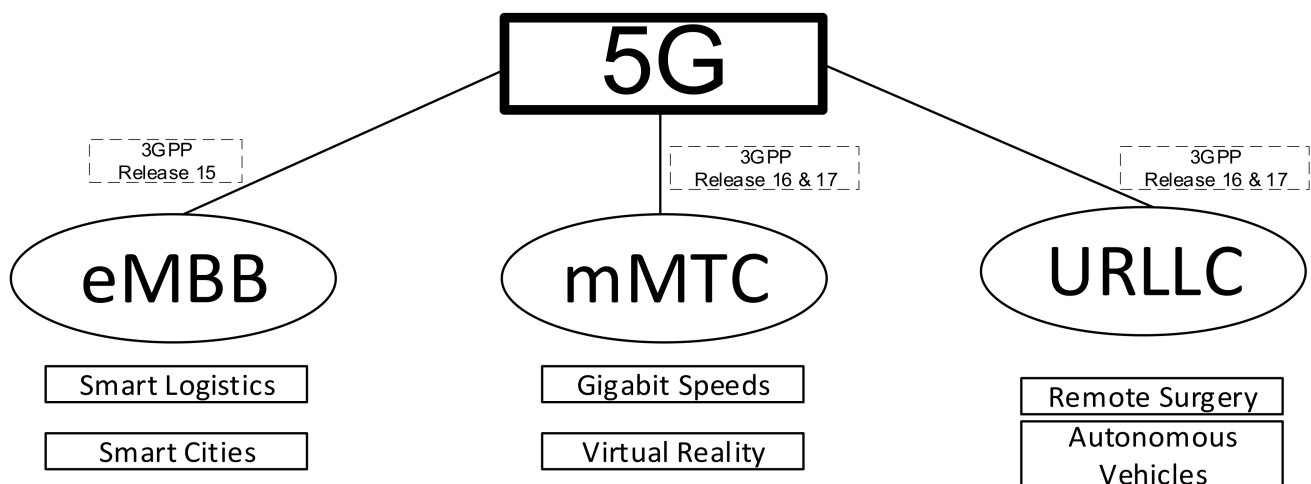


Figure 1. The three groups of 5G use cases.

Standardized in 2018 by the Third Generation Partnership Project (3GPP) Release 15, the initial phase of 5G focused on the improvement of broadband wireless cellular services (eMBB). The other two groups of use cases (mMTC and URLLC) have been defined in the 3GPP release 16 in 2020 to also include the new air interface known as 5G New Radio (NR) and the network slicing concept. Release 17 is expected in 2022, and it will focus on several improvements to 5G, such as network slicing, URLLC, and improved capacity/spectral efficiency, as will be required to support billions of IoT devices needed for smart logistics, smart cities, and autonomous vehicles. Non-Orthogonal Multiple Access (NOMA) is a potential candidate to reach such improved spectral efficiency [3].

In 2005, Quasi-Cyclic Low-Density Parity-Check (QC-LDPC) encoding [4], which is based on the cyclic change of the identity matrix and is also referred to as “structured” LDPC encoding [5], was applied for the first time in the World Interoperability for Microwave Access (WiMAX) standard. The QC-LDPC codes can be defined by a survey size and a base matrix. In 2006, QC-LDPC codes were also recommended for long-term evolution (LTE) channel coding [6]. Later, QC-LDPC codes with the same structure as WiMAX were adopted by IEEE802.11n and IEEE802.11ad because of their remarkable performance and high decoding throughput. In October 2016, QC-LDPC codes were adopted by 3GPP as a data channel encoding scheme for 5G standard because they support very high data transfer rates with low complexity, as opposed to turbo codes utilized in 3G and 4G [7].

Previous work on NOMA focuses mainly on its association with Orthogonal Frequency Division Multiplexing (OFDM) [3,8–11]. Moreover, the study published in [12] focused on the combination of NOMA with massive Multiple-Input Multiple-Output (MIMO), using the Single Carrier with Frequency Domain Equalization (SC-FDE) block transmission technique. This article publishes a holistic study where conventional NOMA and cooperative NOMA are combined with the Low-Density Parity-Check (LDPC) coded massive MIMO (m-MIMO) scheme, SC-FDE and multiple receivers with different levels of complexity and performance, and then studied in different 5G scenarios. Two receivers are used in this study: the Zero Forcing (ZF) receiver and the Maximum Ratio Combiner (MRC) receiver. It is shown that the use of LDPC-coded NOMA with m-MIMO, when combined with conventional or cooperative NOMA, can be utilized with a low level of complexity when the MRC receiver is adopted, whose performances in different scenarios is very close to the ZF receiver (which has much higher computational requirements).

This article is organized as follows: Section 2 describes the system characterization for m-MIMO using SC-FDE transmissions; Section 3 deals with the NOMA concept; Section 4 analyzes the performance results; and Section 5 concludes the article.

2. System Characterization

This article considers both conventional and cooperative NOMA associated with multi-layer MIMO. The number of T transmitting antennas of the multi-layer MIMO corresponds to the number of parallel flows of data (an increase of the symbols rate), while the number of R receiving antennas corresponds to the level of diversity. Multi-layer MIMO requires the number of R receiving antennas to be equal to or higher than the number of T transmitting antennas (see Figure 2). The Quadrature Phase Shift Keying (QPSK) modulation is assumed, associated with SC-FDE signals.

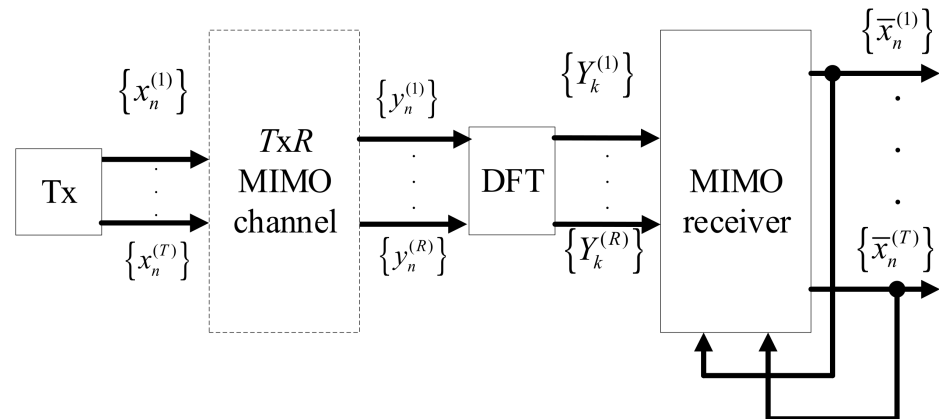


Figure 2. Block diagram of m-MIMO system with SC-FDE signals.

The n th transmitted block, of N data symbols, sent by the t th antenna is denoted as $x_n^{(t)}$, while the received block by the r th antenna is denoted as $y_n^{(r)}$ [13]. The mapping between the time domain signal and the frequency domain signal for the transmitted block is defined as $\{x_n^{(t)}; n = 0, 1, \dots, N - 1\} = IDFT\{X_k^{(t)}; k = 0, 1, \dots, N - 1\}$, i.e., by performing the discrete Fourier transform (DFT) of the time-domain block. Similar mapping for the received block is defined as $\{y_n^{(r)}; k = 0, 1, \dots, N - 1\} = IDFT\{Y_k^{(r)}; k = 0, 1, \dots, N - 1\}$.

After removing the cyclic prefix and assuming a cyclic prefix longer than the overall channel impulse response of each channel, the received frequency-domain signal becomes,

$$\mathbf{Y}_k = [Y_k^{(1)}, \dots, Y_k^{(R)}]^T = \mathbf{H}_k \mathbf{X}_k + \mathbf{N}_k \tag{1}$$

where $\mathbf{X}_k = [X_k^{(1)}, \dots, X_k^{(T)}]^T$, and where \mathbf{H}_k denotes the $T \times R$ channel matrix for the k th subcarrier, with (r, t) th element $\mathbf{H}_k^{(t,r)}$, and where H_k denotes the channel frequency response for the k th subcarrier (which is assumed invariant during the transmission of a given block), and where the mapping between the time domain and frequency domain is defined by $\{H_k; k = 0, 1, \dots, N - 1\} = DFT\{h_n; n = 0, 1, \dots, N - 1\}$. Moreover, \mathbf{N}_k is the frequency-domain block channel noise for that subcarrier.

Assuming a non-iterative receiver, the frequency domain estimated data symbols $\tilde{\mathbf{X}}_k = [\tilde{X}_k^{(1)}, \dots, \tilde{X}_k^{(R)}]^T$ becomes:

$$\tilde{\mathbf{X}}_k = \mathbf{B}_k \mathbf{Y}_k \tag{2}$$

where \mathbf{B}_k is defined in [14] as:

- $\mathbf{B}_k = (\mathbf{H}_k^H \mathbf{H}_k)^{-1} \mathbf{H}_k^H$ for ZF receiver;
- $\mathbf{B}_k = \mathbf{H}_k^H$ for the MRC receiver.

The ZF receiver is a linear algorithm that applies the pseudo-inverse of the frequency response of the channel for each frequency component of the channel. The ZF is very

efficient in removing the intersymbol interference but has the disadvantage of presenting noise enhancement when utilized in post-processing; therefore, it tends to degrade the performance for average to high levels of noise. Moreover, due to the high level of computation that results from the calculation of the pseudo-inverse of the channel, it is very complex, which also represents a high level of battery consumption. The MRC tends to mitigate these limitations due to its simplicity but generates some level of residual interference generated in the decoding process for moderate values of T/R , which can be mitigated by employing an iterative receiver. The iterative receiver implements the following function [14]:

$$\tilde{\mathbf{X}}_k = \mathbf{B}_k^H \mathbf{Y}_k - \mathbf{C}_k \tilde{\mathbf{X}}_k \quad (3)$$

The interference cancellation matrix \mathbf{C}_k can be computed as [14]:

$$\mathbf{C}_k = \mathbf{A}_k^H \mathbf{H}_k - \mathbf{I} \quad (4)$$

where \mathbf{I} is an $R \times R$ identity matrix.

3. The NOMA Concept

In contrast to orthogonal multiple access, NOMA allows for interference between users in the allocation of user resources; therefore, multiple users are served using the same block of resources. To mitigate the effect of interference, interference cancellation schemes such as Successive Interference Cancellation (SIC) are applied. NOMA has demonstrated the potential to handle a large number of connections while offering a superior capacity sum, so understanding NOMA and its use in 5G is extremely important.

Existing NOMA schemes can be classified into two categories: NOMA based on power domain and NOMA based on code domain. The former assigns a unique power level to a user so several users can transmit their signals while sharing the same time-frequency code resources, each using their allocated power. At the receiver side, the signals from the different users can be separated by exploiting the power differences of the users based on SIC. Code domain-based NOMA relies on codebooks, propagation sequences, interleaving patterns, and scrambling sequences to allocate resources non-orthogonally to users.

In power-ordered NOMA, there are two different configurations [3,11,12]: conventional NOMA and cooperative NOMA. Conventional NOMA defines a reference user, and then users' signals with powers higher than that of the reference user are estimated/decoded, regenerated, and cancelled with an SIC before the reference user's signal is detected (see Figure 3). Note that this process is performed by descending order of the interfering users' powers. This sequence leads to better acquisition and more accurate detection of higher power signals. With conventional NOMA, signals of interfering users with power levels lower than that of the reference user are not cancelled, increasing interference and degrading performance. Note that the received power depends on several factors, such as the near-far problem, fading, or power control, though the first one tends to be the most dominant. By adopting cooperative NOMA, all signals of interfering users are cancelled, making the estimation of the signal of the reference user more accurate, improving performance when compared to conventional NOMA.

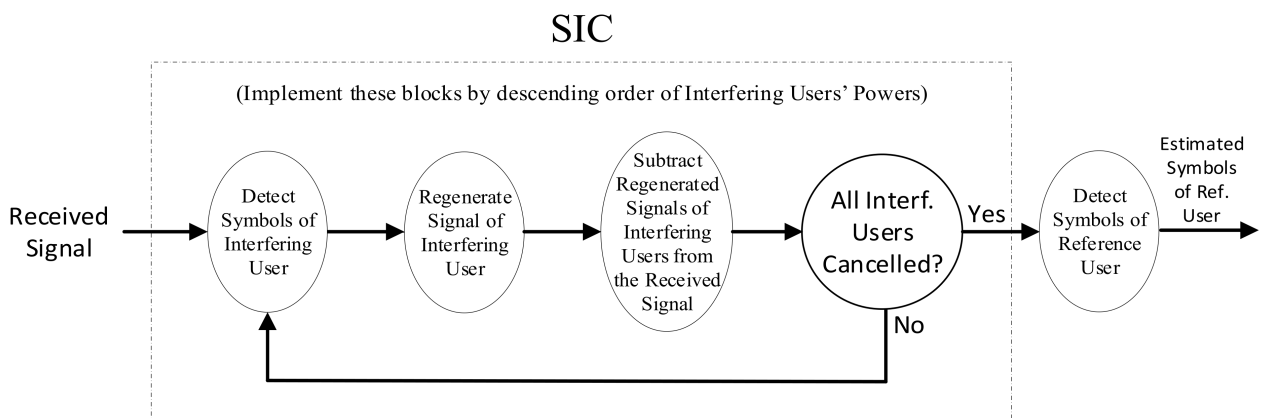


Figure 3. Conventional NOMA and its detection using SIC.

Let us assume that there are a total of U users sharing the spectrum. The received signal at the r th receiving antenna, and n th data symbol, is the cumulative sum of the $\{U; (u = 1 \dots U)\}$ signals that share the spectrum (NOMA signals):

$$y_n^{(r)}(t) = \sum_{u=1}^U y_{u,n}^{(r)}(t) \tag{5}$$

Considering only NOMA users, Equation (1) can be re-written as:

$$\mathbf{Y}_{u,k} = [Y_{u,k}^{(1)}, \dots, Y_{u,k}^{(R)}]^T = \mathbf{H}_{u,k} \mathbf{X}_{u,k} + \mathbf{N}_{u,k} \tag{6}$$

The signal y'_n at the output of SIC for the n th data symbol after the cancellation of the higher power users U' (conventional NOMA) is obtained by:

$$y'_n = y_{u,n} - \sum_{i=1}^{U'} \hat{y}_{i,n} \tag{7}$$

where $\hat{y}_{i,n}$ stands for the estimate of the received signal of the i th interfering user and n th data symbol.

As opposed to conventional NOMA, cooperative NOMA allows the cancellation of interference from all users despite their power levels. This leads to a more accurate estimate of the reference user’s signal, typically achieving performance improvement when compared to conventional NOMA. With cooperative NOMA, reference users relay the signals detected by higher power users over the air, allowing the exploitation of diversity by the other users, which also tends to improve performance. The higher power users can employ an algorithm to combine such relayed signal(s) with the one received directly from the base station [15]. Moreover, in this study, we assume a decode-and-forward relay. A detailed description of cooperative NOMA is provided in [12].

4. Simulation Results and Analysis

This section studies the Bit Error Rate (BER) performance results obtained with Monte Carlo simulations using conventional NOMA and cooperative NOMA, associated with m-MIMO and SC-FDE block transmission techniques. The BER is evaluated as a function of E_b/N_0 , where E_b is the energy of transmitted bits and N_0 is the one-sided power spectral density of the noise. The QPSK modulation was assumed with a block length of $N = 256$ symbols (similar results were observed for other values of N , provided that $N \gg 1$). LDPC codes of length 32,400 were adopted with a code rate of $\frac{1}{2}$. A Rayleigh fading channel was considered with 16 uncorrelated equal power paths. Ideal channel estimation is assumed. A cyclic prefix of $0.125 \mu\text{s}$ was considered. Spatial multiplexing MIMO is assumed (multi-

layer transmission), which means that the number of T transmitting antennas corresponds to the number of parallel flows of symbols, while the number of R receiving antennas is used to exploit diversity. As in the case of the MIMO multi-layer transmission, R needs to be equal to or higher than T for the detection to be possible. In our simulated scenarios, we use at least four times more receiving antennas than transmitting antennas.

Table 1 presents a list of baseline simulations utilized in the different graphics.

Table 1. List of Baselines utilized in simulations.

Baseline 1	Conventional NOMA	MIMO 8×64	w/out LDPC	2 users [0.5 1]
Baseline 2	Conventional NOMA	MIMO 8×64	LDPC	2 users [0.5 1]
Baseline 3	Conventional NOMA	MIMO 8×64	w/out LDPC	3 users [1 0.5 2]
Baseline 4	Cooperative NOMA	MIMO 8×64	w/out LDPC	3 users [1 0.5 2]
Baseline 5	Conventional NOMA	MIMO 8×64	LDPC	3 users [1 0.5 2]
Baseline 6	Cooperative NOMA	MIMO 8×64	LDPC	3 users [1 0.5 2]
Baseline 7	Conventional NOMA	MIMO 8×64	LDPC	4 users [1 0.5 2 4]
Baseline 8	Cooperative NOMA	MIMO 8×64	LDPC	4 users [1 0.5 2 4]
Baseline 9	Conventional NOMA	MIMO 8×256	LDPC	3 users [1 0.5 2]
Baseline 10	Cooperative NOMA	MIMO 8×256	LDPC	3 users [1 0.5 2]

Figure 4 shows the performance results with and without LDPC codes for conventional NOMA with 8×64 MIMO (baselines 1, 2) for two different receivers: the ZF and the MRC. The MFB curve is a way to measure the channel modelled by the sum of delayed and independently Rayleigh-fading rays, which can be viewed as a lower bound. This graphic considers two NOMA users with received power levels [0.5, 1], where the first value in the vector [0.5, 1] (0.5, in this case) corresponds to the power of the reference user and where the other value stands for the power of the interfering user (1, in this case). In this scenario, the power of the interfering user is 3 dB higher than that of the reference user. In this section, we assume that the low power users correspond to those closer to the base station, while higher power users correspond to those further from the base station. Nevertheless, this is only a reference as the received power is not only affected by the near-far problem but also by fading, power control, etc. As previously described, the NOMA receiver includes an SIC, which is utilized to detect and cancel the interference of the higher power users. Therefore, in the current scenario, where the interfering user (potentially further from the base station) has a power 3 dB higher than that of the reference user, that signal is detected first, regenerated, and cancelled/subtracted by the SIC from the overall signal before the reference user's signal is detected. As expected, the results obtained with LDPC are better than those without LDPC for both ZF and MRC. Moreover, when comparing these two receiver types, it is affirmed that they perform similarly. Nevertheless, while the ZF is much more computationally demanding as it requires the computation of the pseudo-inverse of the channel matrix for each frequency component of the channel, the MRC does not. It is worth noting that the MRC is an iterative receiver since it cancels some level of residual interference in each iteration. We only considered four iterations of the MRC receiver as performance improvement beyond that point was negligible.

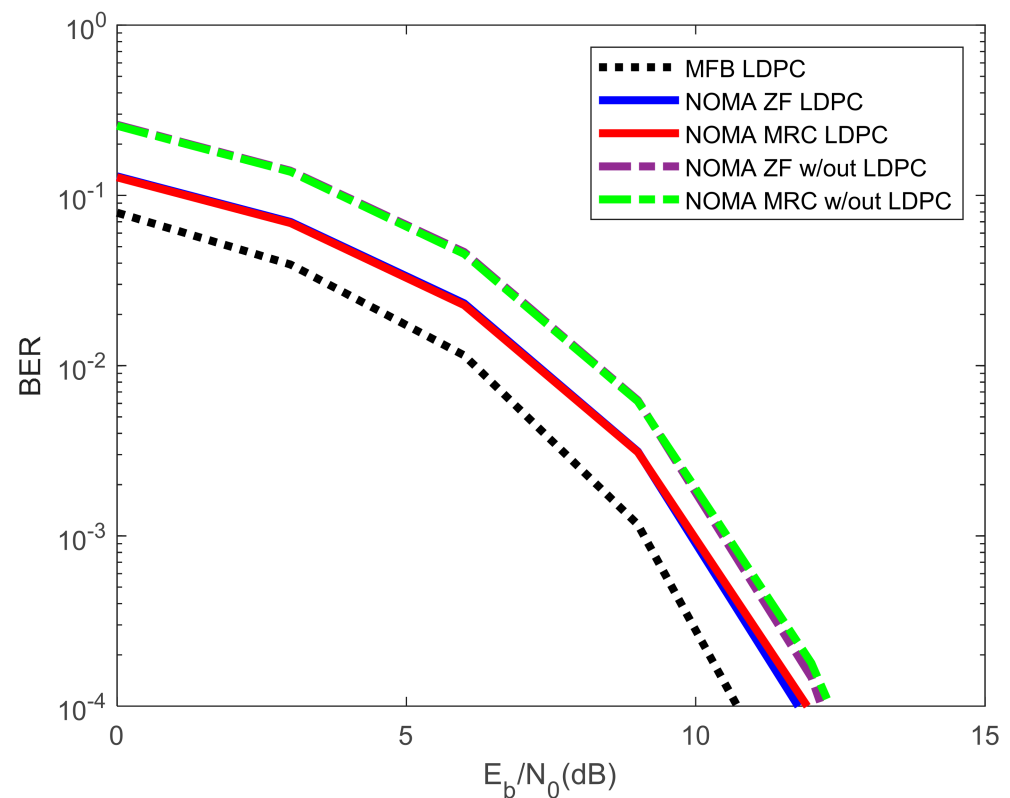


Figure 4. Results for 2 NOMA users with powers [0.5, 1], with 8×64 MIMO (with and without LDPC codes).

Figure 5 shows the performance of conventional NOMA (designated in figures as “NOMA”) and cooperative NOMA (designated in figures as “COOP NOMA”) with 8×64 MIMO with and without LDPC (baselines 3–6) with both ZF and MRC receivers. Three NOMA users with relative powers [1, 0.5, 2] were considered, sharing the spectrum: the reference with the power 1, an interfering user with power 0.5 (i.e., with 3 dB less power than the reference user), and another interfering user with power 2 (i.e., with 3 dB more power than the reference user).

It is known that the sharing of spectrum with regular power-ordered NOMA tends to be limited in terms of performance [16–18] while improving the capacity. This occurs because higher power users are unable to cancel the interference generated by lower power users, representing residual interference. Cooperative NOMA aims to mitigate this limitation by making lower power users relay the signals of higher power users over the air without interference. Weak users are those that tend to be further from the base station (or can also be due to, e.g., fading); thus, the propagation losses are higher. With NOMA, this is mitigated by employing higher transmit power. Therefore, it is assumed that the interfering user with transmit power 0.5 tends to be closer to the base station than the reference user with a transmit power of 1. As can be seen, due to the high level of NOMA interference, the results obtained with conventional NOMA are limited. Cooperative NOMA overcomes such limitations and originates a high-performance improvement with or without LDPC for both receiver types. Cooperative NOMA comprises the cancellation of the interfering signals associated with all users and exploits diversity. Cooperative NOMA considers that the lower power users retransmit the symbols detected by the SIC of higher power users (typically using decode-and-forward in time division multiplexing). These additional signals are utilized by higher power users to exploit diversity as the same signals are also received directly from the base station (assuming downlink). These signals are then combined to improve performance and exploit diversity. Figure 5 shows that a combination of signals performed with cooperative NOMA results in good performance improvement

when compared with conventional NOMA, using both the MRC and ZF receivers, whose performances are close to that of the MFB. It is also viewed that, in this NOMA scenario and for conventional NOMA, the ZF tends to achieve better performance than the MRC for lower levels of noise (higher levels of E_b/N_0). With a high level of interference associated with the non-cancelled interfering NOMA user, the symbol estimates performed in each iteration of the MRC receiver are poor; therefore, it is not able to perform well. On the other hand, even with the noise enhancement typical of the ZF receiver [13], it performs better than that of the MRC. Nevertheless, observing the results with cooperative NOMA, the MRC performs approximately the same as the ZF with and without LDPC.

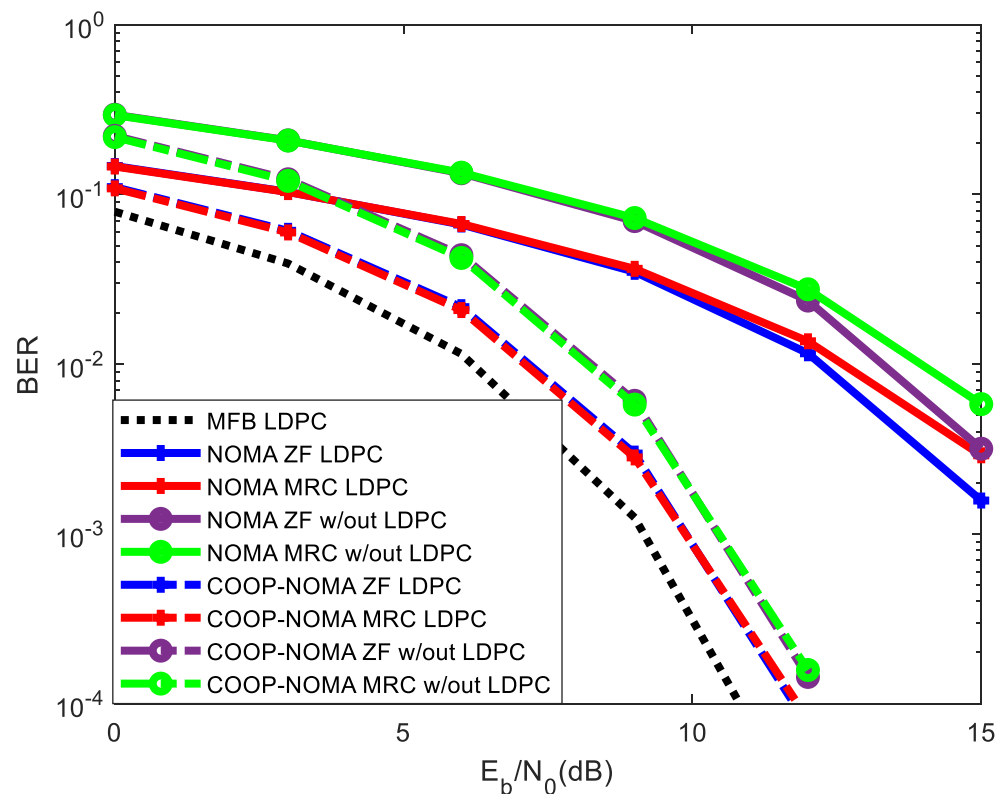


Figure 5. Results for 3 NOMA users with powers [1, 0.5, 2], with 8×64 MIMO (with and without LDPC codes).

Figure 6 shows the performance in a scenario like that of Figure 5 but with four NOMA users with powers [1, 0.5, 2, 4] sharing the spectrum instead of three (baselines 7, 8). A fourth NOMA user with power 4 was added, i.e., with 6 dB more power than that of the reference user. The analysis performed for Figure 5 is also valid for Figure 6. As before, results with LDPC codes are always better than those without, and results with cooperative NOMA are always better than those with conventional NOMA.

Figure 7 shows the performance results for three and four NOMA users sharing the spectrum with 8×64 MIMO and with LDPC codes (baselines 3–8). In the case of three NOMA users, their relative powers are [1, 0.5, 2], while the relative powers of four NOMA users are [1, 0.5, 2, 4], i.e., a fourth user with power 4 was added (6 dB more power than that of the reference user). From Figure 7, we observe that the degradation of performance that results from the addition of the fourth user is residual with either the ZF or the MRC receiver and with conventional NOMA or with cooperative NOMA.

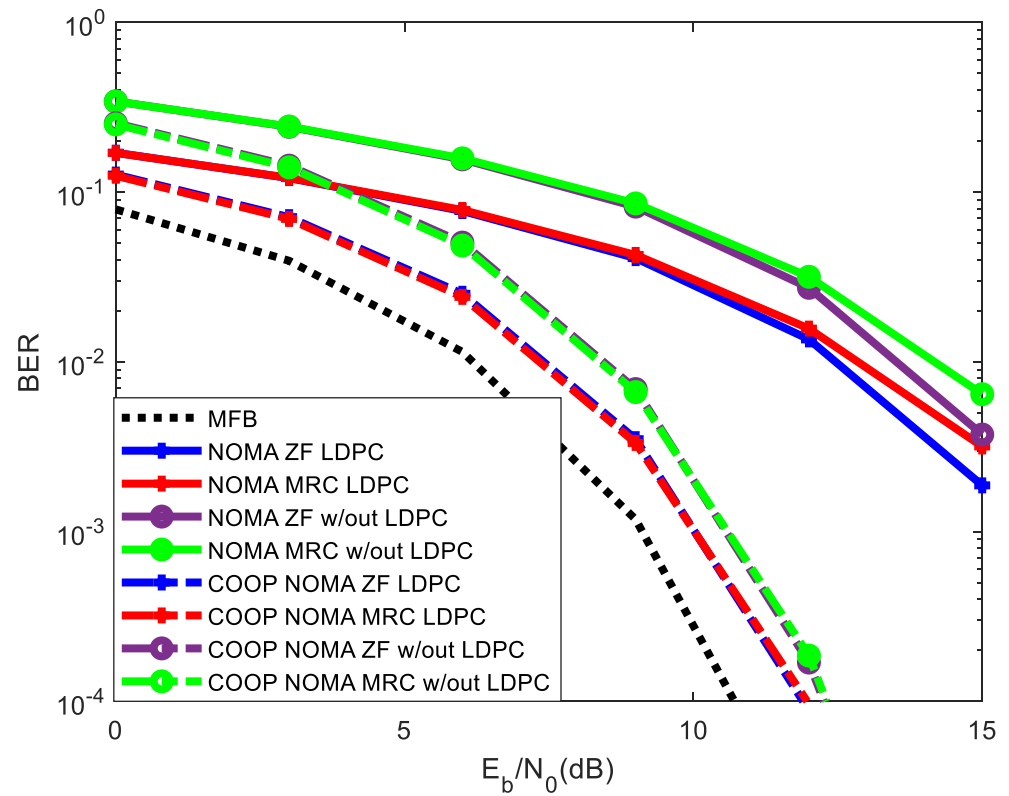


Figure 6. Results for 4 NOMA users with powers [1, 0.5, 2, 4], with 8×64 MIMO (with and without LDPC codes).

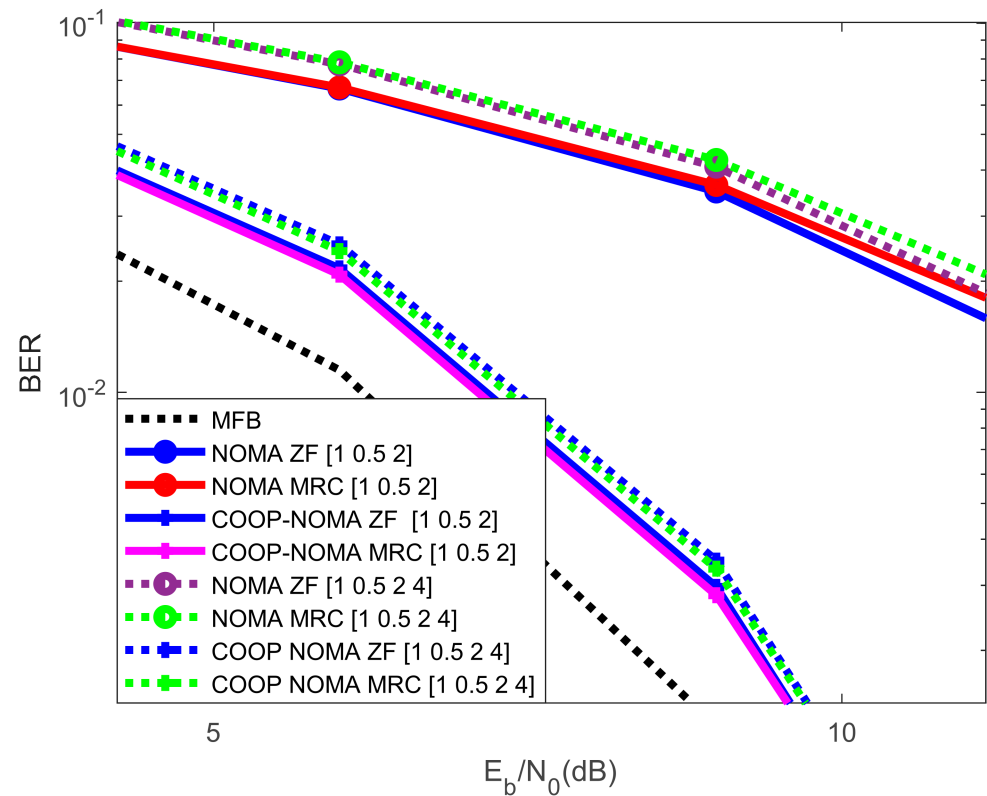


Figure 7. Results for 3 and 4 NOMA users, with 8×64 MIMO, with LDPC codes.

Figure 8 shows the performance results with three NOMA users with powers [1, 0.5, 2], comparing 8×64 versus 8×256 MIMO, with LDPC codes for both conventional NOMA and cooperative NOMA (baselines 5, 6, 9, 10). Since spatial multiplexing MIMO was adopted (also known as multi-layer transmission), the number of transmitting antennas corresponds to the number of parallel flows of data, while the diversity is provided by the number of receiving antennas. Therefore, 8×256 has a diversity four times higher than 8×64 . This translates into an improvement of performance for both conventional NOMA and cooperative NOMA as well as for both receiver types. In the case of conventional NOMA and for 8×64 MIMO, we observe that the ZF performs better than the MRC. Nevertheless, with 8×256 MIMO and conventional NOMA, both receivers perform almost the same while the MRC presents a much lower level of complexity. This occurs because the level of residual interference mitigated by the iterative receiver of the MRC is more precisely estimated and cancelled due to the higher level of diversity provided by the 8×256 MIMO. Moreover, as before, the performance obtained with cooperative NOMA is much better than that of conventional NOMA.

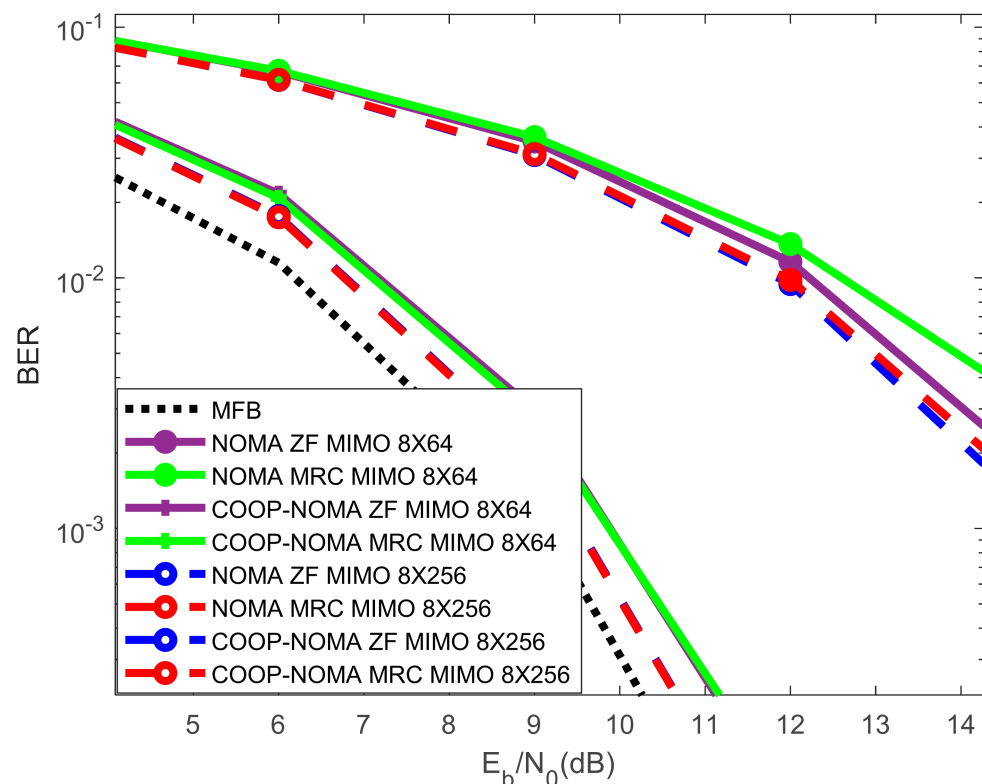


Figure 8. Results for 3 NOMA users with powers [1, 0.5, 2] with 8×64 versus 8×256 MIMO, with LDPC codes.

5. Conclusions

The massive use of IoT devices is demanding more spectrum and alternative ways to share it and/or use it more efficiently. NOMA is a mechanism that allows the spectrum to be shared by different users and is being considered as an option for future 5G evolutions.

This article publishes the results of a study of conventional and cooperative LDPC-coded NOMA with m-MIMO and SC-FDE transmission techniques using two different types of receivers: ZF and MRC. LDPC codes were adopted by 3GPP as the data channel encoding scheme for 5G standard because they support very high data transfer rates with low complexity, as opposed to turbo codes utilized in 3G and 4G.

It was found that cooperative NOMA outperforms conventional NOMA. This occurs because the SIC of conventional NOMA simply suppresses the interference of higher power users, while cooperative NOMA suppresses the interference of all users and exploits

diversity since lower power users retransmit the signals of higher power users over the air. It was also found that while the MRC receiver achieves a performance very close to the ZF receiver, the level of computational demand is significantly reduced, which translates to decreased battery consumption.

Finally, it was concluded that the integration of NOMA with m-MIMO while using LDPC codes, SC-FDE signals and low complexity MRC receivers is a good combination to support future evolutions of 5G.

Author Contributions: All authors contributed equally to the article. All authors have read and agreed to the published version of the manuscript.

Funding: This work is funded by FCT/MCTES through national funds and, when applicable, co-funded EU funds under the project UIDB/EEA/50008/2020.

Acknowledgments: We acknowledge the support of FCT/MCTES, as described above in funding. We also acknowledge the support of Autonoma TechLab for providing an interesting environment to carry out this research.

Conflicts of Interest: The authors declare no conflict of interest.

References

1. Zhou, K.; Liu, T.; Zhou, L. Industry 4.0: Towards future industrial opportunities and challenges. In Proceedings of the 2015 12th International Conference on Fuzzy Systems and Knowledge Discovery (FSKD), Zhangjiajie, China, 15–17 August 2015.
2. Marques da Silva, M.; Guerreiro, J. On the 5G and beyond. *Appl. Sci.* **2020**, *10*, 7091. Available online: <https://www.mdpi.com/2076-3417/10/20/7091> (accessed on 26 August 2021). [[CrossRef](#)]
3. Saraereh, O.A.; Alsaraira, A.; Khan, I.; Uthansakul, P. An efficient resource allocation algorithm for OFDM-based NOMA in 5G systems. *Electronics* **2019**, *8*, 1399. [[CrossRef](#)]
4. Myung, S.; Yang, K.; Kim, J. Quasi-cyclic LDPC codes for fast encoding. *IEEE Trans. Inf. Theory* **2005**, *51*, 2894–2901. [[CrossRef](#)]
5. Xu, J.; Xu, J. Structured LDPC applied in IMT-advanced system. In Proceedings of the International Conference on Wireless Communications Networking and Mobile Computing, Dalian, China, 12–14 October 2008; pp. 1–4.
6. IMT-Advanced Group. IMT-A_LTE+_07061 LDPC coding for PHY of LTE+ air interface. In Proceedings of the IMT-Advanced Group 4th Meeting, Tel Aviv, Israel, 2 September 2007.
7. Li, L.; Xu, J.; Xu, J.; Hu, L. LDPC design for 5G NR URLLC & mMTC. In Proceedings of the 2020 International Wireless Communications and Mobile Computing (IWCMC), Limassol, Cyprus, 15–19 June 2020; pp. 1071–1076. [[CrossRef](#)]
8. Tseng, S.-M.; Tsai, W.-D.; Suo, H.-S. Cross-layer 1 and 5 user grouping/power allocation/subcarrier allocations for downlink OFDMA/NOMA video communications. *Int. J. Commun. Syst.* **2019**, *32*, e4084. [[CrossRef](#)]
9. Wang, S.; Cao, S.; Ruby, R. Optimal power allocation in NOMA-based two-path successive AF relay systems. *EURASIP J. Wirel. Commun. Netw.* **2018**, *2018*, 273. [[CrossRef](#)]
10. Uddin, M.F. Energy efficiency maximization by joint transmission scheduling and resource allocation in downlink NOMA cellular network. *Comput. Netw.* **2019**, *159*, 37–50. [[CrossRef](#)]
11. Ding, Z.; Liu, Y.; Choi, J.; Sun, Q.; Elkashlan, M.; Chih-Lin, I.; Poor, H.V. Application of non-orthogonal multiple access in LTE and 5G networks. *IEEE Commun. Mag.* **2017**, *55*, 185–191. [[CrossRef](#)]
12. Marques da Silva, M.; Dinis, R. Power-ordered NOMA with massive MIMO for 5G systems. *Appl. Sci.* **2021**, *11*, 3541. [[CrossRef](#)]
13. Da Silva, M.M.; Dinis, R. A simplified massive MIMO implemented with pre or post-processing. *Phys. Commun.* **2017**, *25*, 355–362. [[CrossRef](#)]
14. Da Silva, M.M.; Dinis, R.; Guerreiro, J. A low complexity channel estimation and detection for massive MIMO using SC-FDE. *Telecom* **2020**, *1*, 3–17. [[CrossRef](#)]
15. Marques da Silva, M.; Correia, A. Joint multi-user detection and intersymbol interference cancellation for WCDMA satellite UMTS. *Int. J. Satell. Commun. Netw.* **2003**, *21*, 93–117. [[CrossRef](#)]
16. Zhao, Z.; Wang, D.; Zhang, H.; Sang, H. Joint user pairing and power allocation scheme based on transmission mode switching between NOMA-based maximum ratio transmission and MMSE beamforming in downlink MISO systems. *Mob. Inf. Syst.* **2021**, *2021*, 6671371. [[CrossRef](#)]
17. Tseng, S.M.; Chen, Y.F.; Fang, H.H. Cross PHY/APP layer user grouping and power allocation for uplink multi-antenna NOMA video communication systems. *IEEE Syst. J.* **2019**, *14*, 3351–3359. [[CrossRef](#)]
18. Nguyen, H.; Kim, H.; Kang, G.-M.; Nguyen, K.-H.; Bui, V.-P.; Shin, O.-S. A survey on non-orthogonal multiple access: From the perspective of spectral efficiency and energy efficiency. *Energies* **2020**, *13*, 4106. [[CrossRef](#)]